



HAL
open science

Influence of ionic plasticizers on the processing and viscosity of starch melts

Paul Decaen, Agnès Rolland-Sabaté, Gael Colomines, Sophie Guilois, Denis Lourdin, Guy Della Valle, Eric Leroy

► **To cite this version:**

Paul Decaen, Agnès Rolland-Sabaté, Gael Colomines, Sophie Guilois, Denis Lourdin, et al.. Influence of ionic plasticizers on the processing and viscosity of starch melts. *Carbohydrate Polymers*, 2020, 230, pp.1-11. 10.1016/j.carbpol.2019.115591 . hal-02548900

HAL Id: hal-02548900

<https://hal.science/hal-02548900>

Submitted on 15 Jul 2020

HAL is a multi-disciplinary open access archive for the deposit and dissemination of scientific research documents, whether they are published or not. The documents may come from teaching and research institutions in France or abroad, or from public or private research centers.

L'archive ouverte pluridisciplinaire **HAL**, est destinée au dépôt et à la diffusion de documents scientifiques de niveau recherche, publiés ou non, émanant des établissements d'enseignement et de recherche français ou étrangers, des laboratoires publics ou privés.

1 **Influence of ionic liquid plasticizers on the processing and viscosity of starch melts**

2

3 Paul Decaen^{a,b,e}, Agnès Rolland-Sabaté^{b,c,e}, Gaël Colomines^{d,e}, Sophie Guilois^{b,e}, Denis

4 Lourdin^{b,e}, Guy Della Valle^{b,e}, Eric Leroy^{a,e,*}

5

6 a. GEPEA, CNRS, UMR 6144, CRTT, 37, Boulevard de l'Université, 44606 St Nazaire

7 Cedex, France.

8 b. UR1268 Biopolymères Interactions Assemblages, INRA, F-44316 Nantes, France.

9 c. UMR408 Sécurité et Qualité des Produits d'Origine Végétale, INRA, Université

10 Avignon, F-84000, Avignon, France.

11 d. GEPEA, IUT de Nantes, CNRS, UMR 6144, , 2 Avenue du professeur Jean

12 ROUXEL, BP 539, 44475 Carquefou, France.

13 e. IBSM, Rue de la Géraudière, BP 71627, 44316 Nantes cedex 3, France.

14

15 * Corresponding author :

16 email : eric.leroy@univ-nantes.fr ; Phone : +33 240172668 ; Fax +33 240172618

17

18 **Keywords:** Thermoplastic starch, rheology, extrusion, macromolecular degradation, glass

19 transition

20

21

22 **Abstract:**

23 Maize starch was plasticized by glycerol, choline chloride ([Chol][Cl]) and ionic liquids
24 (Choline acetate ([Chol][Ace]), 1-Ethyl-3-methylimidazolium Chloride ([EMIM][Cl]) and 1-
25 Ethyl-3-methylimidazolium acetate ([EMIM][Ace]). Melt rheology at 120°C was assessed
26 with a twin-screw micro-compounder used for processing small quantities (8-10g), and with
27 a capillary rheometer with pre-shearing (Rheoplast). Qualitative agreement was found
28 between shear viscosities obtained by both rheometry devices, showing the interest of the
29 micro-compounder for screening of plasticizers' influence. The lower shear viscosity values
30 were obtained in presence of [EMIM][Ace] whereas [Chol][Cl] led to the largest ones. Rather
31 than processing induced macromolecular degradation, the glass transition temperature
32 depressing effect of the plasticizers was found to better explain viscosity differences. This
33 underlines the strong influence of the nature of the plasticizers on starch melt rheology.
34 Finally, results from extensional viscosity shows the specific influence of [EMIM][Ace],
35 suggesting that this plasticizer could be particularly relevant for thermoplastic starch
36 processing.

37

38 1) Introduction

39 Starch is an abundant, edible, cheap and carbon neutral biopolymer produced worldwide from
40 several different major crops. It is used for a variety of food and non-food applications including
41 bioplastics (Gozzo & Glittenberg, 2009). Native starch granules can be converted into a
42 thermoplastic material by using conventional thermomechanical processing techniques. This
43 requires the presence of small amounts of plasticizers, water and glycerol being the most
44 commonly used. The resulting so called “thermoplastic starch” (TPS) can be shaped into films,
45 foams or bulk parts by compression molding, extrusion or injection molding (H. S. Liu, Xie,
46 Yu, Chen, & Li, 2009). Biodegradable polymer blends and composites can also be produced by
47 melt mixing of TPS with other bioplastics or natural fibers (Averous, 2004). The variations of
48 the viscosity of molten starch with strain and strain rate affect all mixing and shaping processes.
49 Besides flow conditions and deformation modes, the viscous behavior is known to depend on
50 starch botanical origin, plasticizers type and content, and also on processing temperature and
51 particularly previous thermomechanical treatment which affects starch macromolecular
52 structure (Xie, Halley, & Averous, 2012). A minimum specific mechanical energy (SME) input
53 of about 100-200 J g⁻¹ is typically required for a complete destructuring of the native semi-
54 crystalline structure of starch granules under shear (Barron, Bouchet, Della Valle, Gallant, &
55 Planchot, 2001). However, the temperature and SME levels during processing also result in a
56 more or less pronounced degradation of starch macromolecules which strongly affects the
57 viscous behavior (DellaValle, Boche, Colonna, & Vergnes, 1995; Vergnes, Villemaire,
58 Colonna, & Tayeb, 1987). This difficulty is addressed by specific rheometry techniques for
59 measurements under controlled SME conditions: in line (Vergnes, Dellavalle, & Tayeb, 1993);
60 (Horvat, Emin, Hochstein, Willenbacher, & Schuchmann, 2013) or off line with the Rheoplast
61 (Vergnes & Villemaire, 1987). Rheoplast is a reference capillary rheometer with pre-shearing
62 which also allows evaluating extensional viscosity (Della Valle, Vergnes, & Lourdin, 2007), an

63 important property for shaping processes. Concomitantly, models predicting the shear viscosity
64 as a function of temperature, SME, moisture and glycerol content have been developed and
65 validated for starches of different botanical origin (Martin, Averous, & Della Valle, 2003;
66 Vergnes & Villemaire, 1987). In parallel, a few studies have been focused on the viscous
67 behavior of TPS in presence of other plasticizers: small molecules such as formamide (Ning,
68 Yu, Ma, & Han, 2009), citric acid (Wang, Yu, Chang, & Ma, 2007), triethylene glycol, urea
69 and glycerol monostearate (Willett, Jasberg, & Swanson, 1995). A strong influence of
70 plasticizer's structure on starch melt viscosity has been observed (Xie et al., 2012).

71 Room Temperature Ionic Liquids (RTILs) are a new family of starch plasticizers allowing melt
72 processing (Sankri et al., 2010; Xie et al., 2014; Zdanowicz & Szychaj, 2011). RTILs can be
73 tailored by modifying the chemical structure of the cation and anion moieties, opening
74 perspectives for the design of specific plasticizers for starch. However, new RTILs are usually
75 synthesized in small quantities, which makes it difficult to evaluate their potential for starch
76 plasticization. Screening approaches have been proposed using film casting for quantities below
77 1 gram to determine the impact of RTILs on the glass transition temperature (T_g) of TPS, and
78 on film mechanical properties (Colomines, Decaen, Lourdin, & Leroy, 2016). For larger
79 quantities (≈ 10 grams), such properties may be determined on films processed by compression
80 molding (Decaen et al., 2017; Xie et al., 2014; Zdanowicz & Szychaj, 2011) as well as by twin
81 screw micro-compounding (Decaen et al., 2017; Sankri et al., 2010). Such batch process
82 presents the advantage of mimicking twin screw extrusion, with the possibility to quantify SME
83 (Cousin, Berto, Budtova, Kurek, & Navard, 2017; Leroy, Decaen, et al., 2012; Leroy, Jacquet,
84 Coativy, Reguerre, & Lourdin, 2012) and thus to determine its impact on starch macromolecular
85 structure (Decaen et al., 2017). Although the micro-compounder has not been specifically
86 designed for rheological measurements under controlled SME conditions, it has also been
87 shown to be able to evaluate the shear viscosity of non-Newtonian fluids (Yousfi et al., 2014).

88 Hence, it would be interesting to apply it to assess the potential of RTILs for TPS processing at
89 small scale (≈ 10 grams).

90 The aim of the present work is to investigate the effect of different RTIL plasticizers on the
91 viscous behavior of TPS. In this purpose, shear viscosity has been measured at 120 °C with the
92 micro-compounder and with Rheoplast. In complement, Rheoplast allowed estimating the
93 extensional viscosity. The structural changes of RTIL plasticized starches during measurements
94 with both techniques are assessed for their glass transition and macromolecular degradation.

95 2) Experimental

96 2.1) Materials

97 A polystyrene LACQRENE® 6631 was kindly supplied by Arkema. Regular corn starch was
98 purchased from Tate & Lyle (Meritena 100). It has an amylose content of 27%, a weight-
99 average molar mass $\bar{M}_w \approx (198 \pm 10) \times 10^6 \text{ g.mol}^{-1}$ and a dispersity $\bar{M}_w/\bar{M}_n = (2.1 \pm 0.1)$. The
100 macromolecular characterization techniques are described in detail below. Note that in the
101 present article, a great attention will be paid to the influence of melt processing on the
102 degradation of this pristine macromolecular structure, affecting molar masses and rheology.

103 Glycerol was purchased from Sigma-Aldrich. Potassium acetate and choline chloride
104 ([Chol][Cl]) were purchased from Sigma-Aldrich. This salt, although not being a RTIL, is an
105 efficient plasticizer of starch (Abbott, 2009; Decaen et al., 2017; Zdanowicz & Sychaj, 2011).

106 The RTIL used are: i) Choline acetate ([Chol][Ace]), synthesized by ion exchange as described
107 in detail in a previous paper (Colomines et al., 2016); ii) 1-Ethyl-3-methylimidazolium Chloride
108 ([EMIM][Cl] ; and iii) 1-Ethyl-3-methylimidazolium acetate ([EMIM][Ace]) both purchased
109 from Solvionic (Toulouse, France).

110 The four different ionic plasticizers ([Chol][Cl] ; [Chol][Ace] ; [EMIM][Cl] and [EMIM][Ace])
111 and glycerol were premixed with the starch powder containing 12% of water using a kneading

112 machine. The dry basis plasticizer content was fixed to 23%. These premixed powders, were
113 stored 24h at 4 °C before melt processing and rheological characterization.

114 2.2) Processing and rheological characterization with the micro-compounder

115 A micro-compounder (Haake Minilab, Thermo Scientific GmbH, Karlsruhe, Germany) was
116 used for small scale evaluation of shear viscosity. This batch device, with a working volume
117 $V=7 \text{ cm}^3$, makes it possible to simulate extrusion for a typical quantity of 8-10 g of TPS. It
118 consists of a conical twin screw system ($L_{\text{screw}} = 12 \text{ cm}$) with a slit shaped back flow channel
119 ($64 \times 10 \times 1.5 \text{ mm}^3$). The material can be recirculated during the desired residence time before
120 being extruded through the exit die.

121 *2.2.1) Rheometry*

122 Two pressure sensors located in the recirculation channel allow estimating the shear stress. The
123 shear rate is determined on the assumption that the flow rate in the recirculation channel, Q
124 [$\text{m}^3 \cdot \text{s}^{-1}$], is proportional to the screw speed N (rpm):

$$125 \quad Q = C \cdot N \quad (1)$$

126 Where: C is a calibration constant which depends on the screw type (co-rotating or counter
127 rotating) and can vary slightly ($\pm 20\%$) with the polymer type (Yousfi et al., 2014). In our case,
128 it was obtained by calibration with a polystyrene (LACQRENE® 6631) of known rheological
129 behavior, as explained below.

130 Since the backflow channel's thickness ($h= 1.5 \text{ mm}$) is small in comparison to its width ($w =$
131 10 mm), the shear stress τ_w at the wall of the channel can be evaluated as follows (Son, 2007):

$$132 \quad \tau_w = \frac{h \times \Delta P}{2 \times \Delta L} \times \left(\frac{1}{\frac{h}{w} + 1} \right) \approx \frac{h \times \Delta P}{2 \times \Delta L} \quad (2)$$

133 Where $\Delta L = 64 \text{ mm}$ is the distance between the pressure sensors.

134 The apparent shear rate is given by (Son, 2007):

$$135 \quad \dot{\gamma}_{app} = \frac{6 \times Q}{w \times h^2} \quad (3)$$

136 A power law is assumed for the shear rate dependence of TPS shear viscosity η :

$$137 \quad \eta = K \times \gamma^{n-1} \quad (4)$$

138 The pseudo plasticity index n is obtained from the slope of the plot of $(\log \tau)$ vs. $(\log \dot{\gamma}_{app})$. This
139 allows applying the modified Rabinowitsch correction taking into account the dimensions of
140 the slit backflow channel (Son, 2007):

$$141 \quad \dot{\gamma}_w = \dot{\gamma}_{app} \times \frac{2}{3} \left(\frac{b^*}{f^*} + \frac{a^*}{f^*} \times \frac{1}{n} \right) \quad (5)$$

142 Where: $a^* = 0.3781$, $b^* = 0.8745$ and $f^* = 0.8351$ for $(h/w) = 0.15$.

143 Finally the viscosity is given by:

$$144 \quad \eta = \frac{\tau_w}{\dot{\gamma}_w} \quad (6)$$

145 2.2.2) Calibration with a commercial polystyrene

146 To determine the value of parameter C in equation (1), a commercial polystyrene
147 (LACQRENE® 6631) was used. This polymer was chosen because around 180 °C – 200 °C, it
148 has a viscosity range close to that of TPS at 120 °C, while not being sensitive to SME. The
149 viscosity of LACQRENE® 6631 follows a Cross/Carreau law:

$$150 \quad \eta = \frac{\eta_0}{1 + \left(\frac{\eta_0 \cdot \dot{\gamma}}{\tau^*} \right)^{1-n}} \quad (7)$$

151 According to the MOLDFLOW™ database the parameters are given by:

$$152 \quad \eta_0 = D_1 e^{\left[\frac{-A_1(T-T^*)}{A_2+(T-T^*)} \right]} \quad (8)$$

$$153 \quad T^* = D_2 + D_3 \cdot P \quad (9)$$

154
$$A_2 = \tilde{A}_2 + D_3 \cdot P \quad (10)$$

155 Where : $D_3=0$ (Pa.K⁻¹) ; $\tilde{A}_2=51.6$ (K) ; $D_2 = 373.15$ (K) ; $A_1=23.629$; $D_1=2.75 \cdot 10^{10}$ (Pa.s) ;
156 $\tau^*=18549$ (Pa) et $n=0.3195$.

157 Therefore, the theoretical flow curve can be calculated using equations 7-10, and the constant
158 C in equation (1) is derived by matching experimental measurements from the micro-
159 compounder, treated through equations 3-6, with this theoretical flow curve.

160 Calibration measurements were conducted at 180 °C and 200 °C with LACQRENE® 6631.
161 The material was introduced in the micro-compounder at 100 rpm. After complete filling, the
162 rheological characterization step was started: the screw speed N was decreased step by step
163 down to 5 rpm. Each step was maintained during approximately 20 s allowing the pressure drop
164 (ΔP) between the two pressure sensors in the back flow channel to stabilize. The recorded
165 values (N, ΔP) were used for viscosity calculations and adjustment of the constant C.

166 *2.2.3) Processing and rheological characterization experiments with TPS*

167 The starch/plasticizer premixed powders were introduced at 120 °C with a screw speed of 100
168 rpm in co-rotating mode with recirculation and melt-processed during 150 seconds before the
169 rheological characterization was started: measurements were first conducted by decreasing the
170 screw speed N by steps of 10 rpm from 100 to 10 and then at 5 rpm. Then, a second series of
171 measurements was performed starting at 5 rpm and increasing to 25, 50, 75 and 100 rpm. Each
172 step was maintained during approximately 30 s. The total duration of one experiment was
173 typically 700 s. The average pressure drop (ΔP) between the two pressure sensors in the back
174 flow channel was calculated for each screw speed (N). The (N, ΔP) values were used for the
175 evaluation of shear viscosity, using the constant C obtained with LACQRENE® 6631. In order
176 to evaluate the influence of processing on the calculated viscosity, two sets of (N, ΔP) values

177 were considered: those obtained for decreasing N (100; 90 ...10, 5) and those for increasing N
178 (5, 25, 50, 75, 100).

179 During such measurements, an increase of SME, cumulated by the recirculating TPS, takes
180 place. An average SME value was thus evaluated by performing a second series of experiment
181 at 120 °C with a constant screw speed of 100 rpm, for a total residence time of 300 s and without
182 rheological measurement. The engine torque signal was recorded allowing the calculation of
183 the Specific Mechanical Energy (SME) ($J g^{-1}$) input:

$$184 \quad SME = \int_0^t \frac{T \cdot 2\pi \cdot N \cdot dt}{M \cdot 60} \quad (11)$$

185 Where: T is the torque [N m], N is the screw speed [min^{-1}], t, the residence time [s], and M, the
186 mass of TPS in the micro-compounder [g].

187 2.3) Rheoplast processing and rheological characterization.

188 The total quantity of starch/plasticizer premixed powder required for rheological
189 measurements with Rheoplast is typically 150-300g (compared to 8-10g for the micro-
190 compounder). This specific capillary rheometer has been used to determine the shear viscosity
191 of molten maize starch, whilst simulating extrusion treatment under controlled
192 thermomechanical conditions (Vergnes & Villemaire, 1987). In this purpose, the powdery
193 material is introduced by batches of 15 g in the machine: the piston used to push the material
194 and inject it through the capillary die can also rotate at a constant set speed, like in a Couette
195 geometry, prior to moving down. Hence, it allows imposing to the material a well-defined shear
196 during a given time, and then a fixed amount of SME. In the present case, inner piston rotation
197 speed was 100 rpm. Barrel temperature was adjusted through two heating elements at 110 °C
198 in the Couette geometry and 115 °C in the injection reservoir, for all TPS formulations. Sample
199 temperature, measured before the capillary die was 120 °C (+/-2 °C). This temperature value
200 was selected to avoid any thermal degradation, possible in the case of Choline based IL. Four

201 cylindrical dies of diameter 2 mm and various L/D ratio values (0.05, 4, 8 and 16) were used.
202 The conical entrance angle was 90° . Once pressure P values have been measured for different
203 values of apparent shear rate $\dot{\gamma}_a$ in the interval $[0.64, 166 \text{ s}^{-1}]$, starch/plasticizer premixed
204 powder was added in the hopper and the operation was repeated until obtaining three pressure
205 profiles $P(\dot{\gamma}_a)$ within an interval of $\pm 10\%$. From these pressure profiles, Bagley end
206 corrections were performed in order to derive the wall shear stress τ_w . The true wall shear rate
207 $\dot{\gamma}_w$ was then determined after performing Rabinowitsch corrections, according to conventional
208 capillary rheometry treatment, as indicated by Della Valle et al. (Della Valle et al., 2007).
209 Elongational viscosity was derived from entrance pressure drop according to the analysis
210 proposed by (Cogswell, 1972).

211 2.4) Characterization of TPS samples

212 The samples collected for each Rheoplast experiment and for the second series of processing
213 experiments with micro-compounder were characterized in order to determine the glass
214 transition temperature and the macromolecular degradation associated to the measured melt
215 viscosity.

216 *2.4.1) Glass transition temperature*

217 Differential scanning calorimetry (DSC) was used to determine the glass transition temperature
218 T_g of the extruded samples with a DSC Q100 apparatus (TA Instruments, New Castle, DE,
219 USA). Stainless steel sealed pans prevented any water loss during tests. A scan was then
220 performed from -60 to $100 \text{ }^\circ\text{C}$ at $10 \text{ }^\circ\text{C min}^{-1}$. T_g was defined as the midpoint of the heat
221 capacity jump on thermograms.

222 *2.4.2) Macromolecular characterizations*

223 High-Performance Size-Exclusion Chromatography coupled with Multi-Angle Laser Light
224 Scattering and Differential Refractive Index detection (HPSEC-MALLS) was used to

225 determine the macromolecular characteristics of the samples. Collected plasticized starch
226 samples (and native starch used as a reference) were first solubilized in dimethylsulfoxide,
227 precipitated with ethanol and dried. They were then solubilized in filtered Millipore water (0.1
228 μm , Durapore GV membrane from Millipore) at a concentration of 0.5 g L^{-1} by microwave
229 heating under pressure, as described in previous works (Rolland-Sabate, Amani, Dufour,
230 Guilois, & Colonna, 2003; Sciarini et al., 2015). After filtration through $5 \mu\text{m}$ Durapore™
231 membranes (Waters, Bedford, MA, USA), $100 \mu\text{L}$ of each solution was injected into the
232 HPSEC-MALLS system. Sample recoveries were calculated from the ratio of the initial mass
233 and the mass after filtration (Rolland-Sabate et al., 2003). The HPSEC-MALLS- equipment
234 and the method used were the same as that described previously (Sciarini et al., 2015). The SEC
235 column was a Shodex® KW-802.5 (8 mm ID×30 cm) together with a KW-G guard column (6
236 mm ID×5 cm) both from Showa Denko K.K. (Tokyo, Japan), maintained at $30 \text{ }^\circ\text{C}$. The two on-
237 line detectors were a Dawn® Heleos® MALLS system fitted with a K5 flow cell and a GaAs
238 laser, ($\lambda = 658 \text{ nm}$), supplied by Wyatt Technology Corporation (WTC, Santa Barbara, CA,
239 USA,) and an RID-10A refractometer from Shimadzu (Kyoto, Japan). Sample recovery rates
240 were calculated from the ratio of the mass eluted from the column (integration of the
241 refractometric signal) and the injected mass (Rolland-Sabate et al., 2003).

242 The weight-average and the number average molar masses (\overline{M}_w , \overline{M}_n) and the dispersity (\overline{M}_w
243 $/\overline{M}_n$) were established using ASTRA® software from WTC (version 6.1 for PC), as
244 previously described (Rolland-Sabate, Mendez-Montecalvo, Colonna, & Planchot, 2008). A
245 value of 0.146 mL g^{-1} was used as the refractive index increment (dn/dc) for glucans and the
246 normalization of photodiodes was achieved using a low molar mass pullulan standard (P20).

247

248 3) Results and discussion

249 3.1) Specific Mechanical Energy and induced macromolecular degradation

250 The SME values determined during rheological testing with the Rheoplast and Micro-
251 compounder are given in **Table 1**. Also reported in Table 1 are the values of T_g measured on
252 plasticized starch samples, and their macromolecular characteristics determined from HPSEC-
253 MALLS chromatograms (**Fig. 1**). It is noteworthy that solubilization rate through the HPSEC-
254 MALLS system is between 91 and 100%, except for the plasticized starch obtained by
255 Rheoplast with glycerol (80%), and elution recovery rate is between 86 and 100%. These high
256 recovery rate values show that the macromolecular characterizations by HPSEC-MALLS are
257 representative of the processed TPS samples.

258 The SME values obtained with the micro-compounder are generally higher than with the
259 Rheoplast (except for [EMIM][Cl]) but all average values fall in the 100-500 J g⁻¹ range which
260 is generally expected to allow an efficient starch granule destructuring, without too strong molar
261 mass degradation (Vergnes et al., 1987). Indeed the macromolecular characteristics confirm a
262 moderate degradation of starch macromolecules, stronger in the case of micro-compounder due
263 to higher SME. As reported in **Table 1**, TPS samples processed with Rheoplast present \overline{M}_w
264 values ranging from 4.33×10^7 to 1.25×10^8 g mol⁻¹; while samples processed with micro-
265 compounder have lower \overline{M}_w values ranging from 5.0×10^6 to 1.69×10^7 g mol⁻¹. Compared to
266 native starch ($\overline{M}_w = 1.98 \times 10^8$ g mol⁻¹), the decrease of molar mass seems large, nevertheless
267 all \overline{M}_w values remain higher than 10^6 g mol⁻¹. This is particularly important since for \overline{M}_w
268 values lower than 10^6 g mol⁻¹, the glass transition temperature (T_g) of TPS can become
269 dependent of molar mass, as observed in previous studies in the case of hydrolyzed pea starch
270 (Lafargue, Pontoire, Buleon, Doublier, & Lourdin, 2007). It is also noteworthy that for maize
271 starch, the entanglement molecular weight is close to 10^5 g mol⁻¹ (Carriere, 1998). So, despite

272 macromolecular degradation, macromolecular masses weights remain much higher than this
 273 critical value.

Plasticizer of starch	HPSEC MALLS			Processing	DSC	
	\overline{M}_w (10^6 g mol^{-1})	\overline{M}_n (10^6 g mol^{-1})	$\overline{M}_w / \overline{M}_n$	EMS (J g^{-1})	T_g ($^{\circ}\text{C}$)	Water (%)
Micro-compounder						
Glycerol	16.1	4.6	3.5	443 \pm 50	12	13
[Chol][Cl]	11.0	6.6	1.7	322 \pm 50	15	15
[Chol][Ace]	5.0	2.9	1.8	362 \pm 50	5	16
[EMIM][Cl]	10.8	5.8	1.9	114 \pm 50	-6	12
[EMIM][Ace]	16.9	11.6	1.5	199 \pm 50	0	16
Rheoplast						
Glycerol	43.3	9.6	4.5	140 \pm 50	not measured	
[Chol][Cl]	97.2	13.3	7.3	140 \pm 50		
[Chol][Ace]	104.0	14.6	7.1	130 \pm 50		
[EMIM][Cl]	125.0	19.4	6.5	250 \pm 50		
[EMIM][Ace]	57.5	10.5	5.5	170 \pm 50		
Native starch*	198.0	93.0	2.1	–		

274 **without process. Standard deviations were about 5% for molar masses*

275 **Table 1:** SME values and Macromolecular characteristics: Weight-average and number-
 276 average molar masses (\overline{M}_w , \overline{M}_n), dispersity ($\overline{M}_w / \overline{M}_n$) obtained by integrating the HPSEC-
 277 MALLS signals for the whole population of macromolecules present in the sample, for corn
 278 starch samples processed with different plasticizers and for native corn starch.

279

280

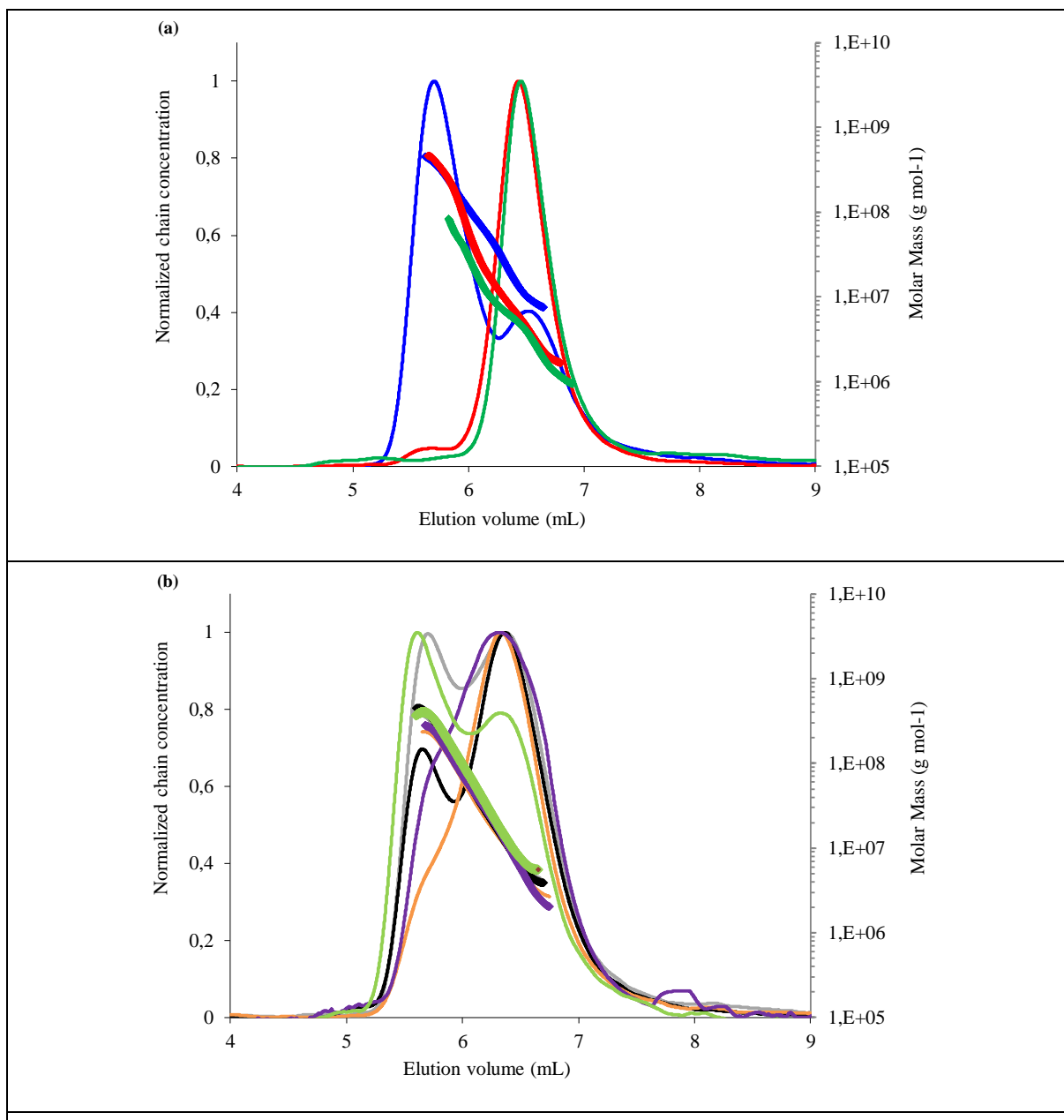


Figure 1: Chromatograms of native and processed corn starches: Normalized chain concentration obtained from the DRI answer (thin lines) and molar masses (thick lines) versus elution volume. (a) Native corn starch (blue) and TPS processed with the micro-compounder, plasticized with glycerol (red) and [Chol][Ace] (green), (b) TPS processed with Rheoplast, plasticized: with glycerol (orange), [Chol][Cl] (black), [Chol][Ace] (grey), [EMIM][Cl] (green) and [EMIM][Ace] (purple).

282 T_g values measured for the samples processed with the micro-compounder are reported in **Table**
283 **1**: no correlation can be drawn neither with \overline{M}_w values, nor with water content values, thus
284 indicating that the the nature of the plasticizer affects T_g value. As in previous work on TPS
285 films obtained by casting from water solutions (Colomines et al., 2016), imidazolium ionic
286 liquids lead to larger T_g depression than glycerol and cholinium ionic liquids (**Table 1**).

287 However, a closer look at chromatograms (**Fig. 1**) indicates that the macromolecular structure
288 of TPS and dispersity are strongly affected by both processing/SME and plasticizer nature. If
289 we consider first native starch as a reference, the chromatogram shows a main peak at 5.7 mL
290 corresponding to the amylopectin population and a peak at 6.45 mL corresponding to the
291 amylose population (**Fig. 1a**).

292 The chromatograms of plasticized starches exhibit peaks shifted to higher elution volumes,
293 showing a decrease of amylopectin macromolecular size. This decrease has already been
294 observed for extruded starches (W. C. Liu, Halley, & Gilbert, 2010; Logie, Della Valle,
295 Rolland-Sabate, Descamps, & Soulestin, 2018; van den Einde, Akkermans, van der Goot, &
296 Boom, 2004; van den Einde, Bolsius, et al., 2004) and starches processed with ionic liquids
297 (Decaen et al., 2017; Sankri et al., 2010; Sciarini et al., 2015). It results from the amylopectin
298 degradation into dextrans and has been attributed to the larger sensitivity of this macromolecule
299 to shear, compared with the one of amylose. However, a significant difference can be observed
300 depending on the processing conditions:

- 301 • For TPS samples processed with the micro-compounder: while the initial amylopectin
302 peak (between 5.5 and 6 mL) is still present after processing with glycerol, it completely
303 disappears after processing with the ionic liquids as illustrated in the case of [Chol][Ace]
304 (**Fig. 1a**). The curves obtained with the other ionic liquids are not shown for the sake of
305 clarity but in all cases, a single peak is obtained, between 6 and 7 mL, resulting in a low

306 dispersity for starches processed with ionic liquids ($\overline{M}_w / \overline{M}_n = 1.5 - 1.9$) compared to
307 native and glycerol plasticized starches (4.7 and 3.5 respectively, **Table 1**).

308 • For samples plasticized on Rheoplast, the initial amylopectin peak is still present in the
309 chromatograms, yet in different proportions depending on the plasticizer (**Fig. 1b**). In
310 all cases, Rheoplast processing with ionic liquids results in a high dispersity (6.5 to 7.3)
311 compared to native starch and glycerol plasticized starch (4.5, **Table 1**). The latter
312 exhibits the highest amylopectin degradation (the lowest amount of residual
313 amylopectin, the lowest average molar mass). Conversely, the least amylopectin
314 degradation is observed for [EMIM][Cl].

315 These results show that besides processing conditions and SME, the nature of the plasticizer
316 influences macromolecular degradation.

317

318 3.2) Shear viscosity

319 **Fig. 2** shows the calibration curves obtained by the micro-compounder for the polystyrene
320 reference and the shear viscosity curves obtained TPS plasticized with glycerol (considered as
321 a reference plasticizer) with the micro-compounder and Rheoplast. The adjusted value of $C =$
322 $6 \cdot 10^{-10} \text{ m}^3 \text{ s}^{-1} \text{ rpm}^{-1}$ (equation 2) allows fitting of the experimental points to the Cross-Carreau
323 reference model describing polystyrene viscosity (**Fig. 2a**) for both temperatures (180 °C and
324 200 °C). As expected, the TPS plasticized with glycerol displays the classical viscous behavior
325 (**Fig. 2b**) described by the power law (equation 4). The shear viscosity values calculated from
326 micro-compounder measurements cover a smaller range of shear rate than the one covered by
327 the Rheoplast. As shown in **Table 2**, the viscosity values at 10 s^{-1} are rather close: 10.9 kPa s
328 for Rheoplast and 7.5 kPa s for micro-compounder operated at decreasing screw speed. The
329 pseudo plasticity index values are the same ($m=0.28$), while the values of consistency index K
330 are 57 kPa s^{n-1} with Rheoplast and 39 kPa s^{n-1} with micro-compounder. The lower values

331 obtained with the latter may be explained by the significantly higher SME and thus, stronger
332 induced macromolecular degradation, as discussed previously (**Table 1**), and in agreement with
333 the results of Martin et al. (Martin et al., 2003). Looking more precisely at the results obtained
334 with the micro-compounder, viscosity measurements with decreasing N (screw speed) lead to
335 lower values than those obtained when increasing N. This result was observed for all other
336 plasticizers, and it suggests that viscosity increases during measurement, as explained in the
337 experimental section (2.2.3). It may be explained by water loss during measurement, the
338 influence of which balances the strong sensitivity of consistency to SME (Martin et al., 2003).

339 **Fig. 3** shows the shear viscosity curves obtained with micro-compounder and Rheoplast. For
340 clarity's sake, they are presented according to ionic plasticizers: Acetate salts (**Fig. 3a**) and
341 Chloride salts (**Fig. 3b**). In both cases, the imidazolium ionic liquids lead to the lower viscosity
342 values. Besides, all viscosity values at 10 s^{-1} are lower than for glycerol plasticized starch
343 (**Table 2**) except for [Chol][Cl] in micro-compounder measurements. Actually, for this
344 plasticizer, it was not possible to obtain stable pressure data during the decreasing screw speed
345 steps. Therefore, the viscosity values were obtained for the increasing screw speed test. In this
346 case, the high viscosity obtained may be explained by water loss, and the possible crystallization
347 at low water content of [Chol][Cl], which is not a RTIL and has a dry melting point at $302 \text{ }^\circ\text{C}$.

348 Whatever the variations, the consistency values of the TPS obtained for the other plasticizers,
349 with both Rheoplast and micro-compounder, rank in the same following order:

$$350 \quad K_{[\text{Chol}][\text{Cl}]} > K_{\text{Glycerol}} > K_{[\text{Chol}][\text{Ace}]} > K_{[\text{EMIM}][\text{Cl}]} > K_{[\text{EMIM}][\text{Ace}]}.$$

351 This agreement between the results found with the two different equipment suggest that the
352 micro-compounder has potential as a rheometrical tool, for testing TPS when only small
353 quantites of material are available. The values of pseudo-plasticity index n slightly differ from
354 one equipment to another, in the case of imidazolium ionic liquids. This difference is likely due
355 to the slight uncertainty in the measurements with the micro-compounder, because of the

356 narrow range of shear rate values used to determine n from the slope of the curve ($\log \tau$) vs.
 357 ($\log \dot{\gamma}_{app}$), rather than to a real influence of this plasticizer on starch rheological behavior in
 358 these thermomechanical conditions.

Plasticizer	Rheoplast			Micro-compounder		
	K (kPa s)	n	η at 10 s^{-1} (KPa s)	η at 10 s^{-1} (KPa s)	K (kPa s)	n
Glycerol	57	0.28	10.9	7.5	39	0.28
[Chol][Cl]	65	0.18	9.8	11.8	74	0.20
[Chol][Ace]	51	0.30	10.2	7.3	35	0.32
[EMIM][Cl]	44	0.21	7.1	4.0	19	0.33
[EMIM][Ace]	31	0.23	5.2	3.9	18	0.33

359

360 **Table 2:** Comparison of shear viscosity and power law values obtained with the Rheoplast
 361 and the Micro-compounder for the different TPS.

362

363

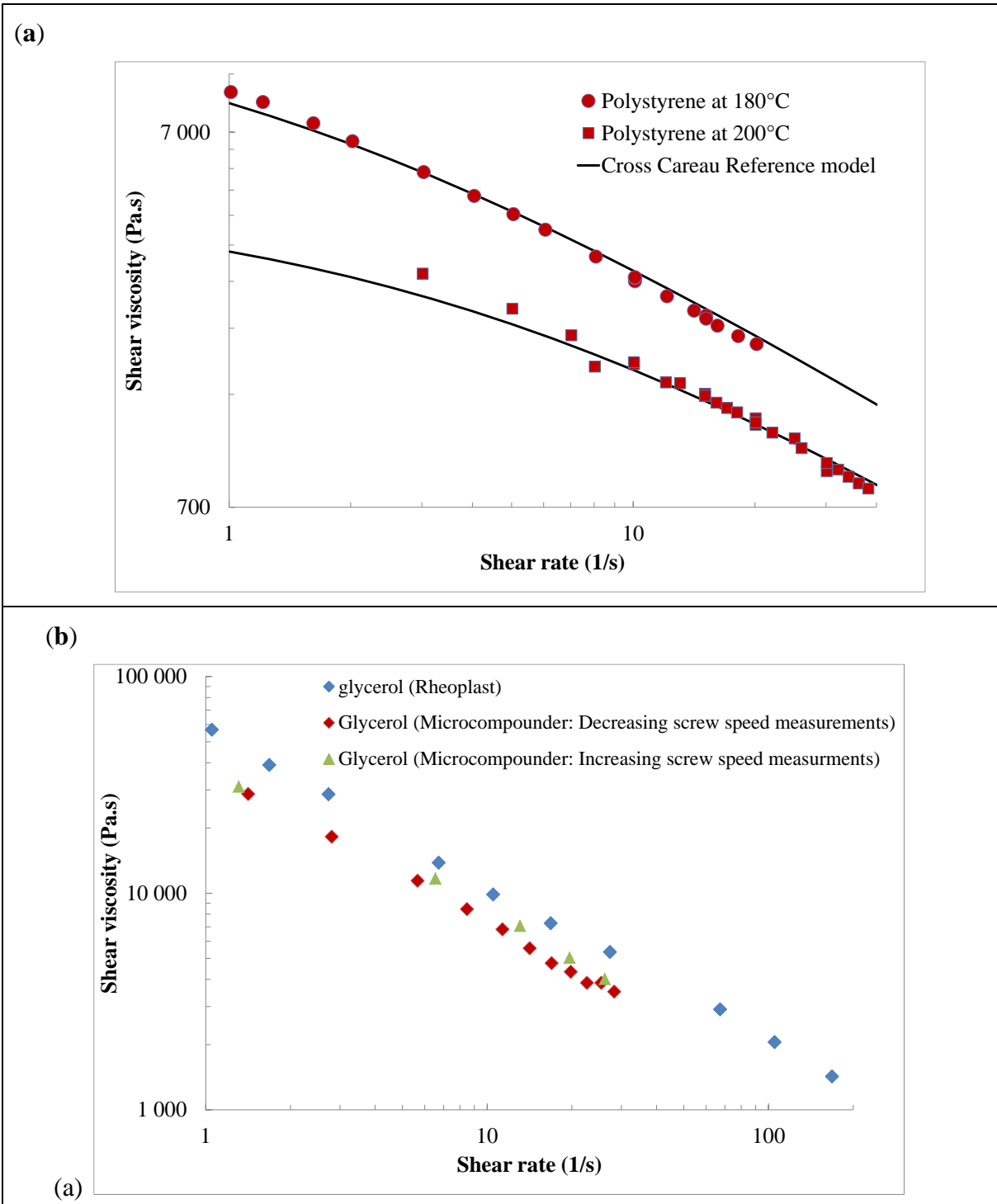
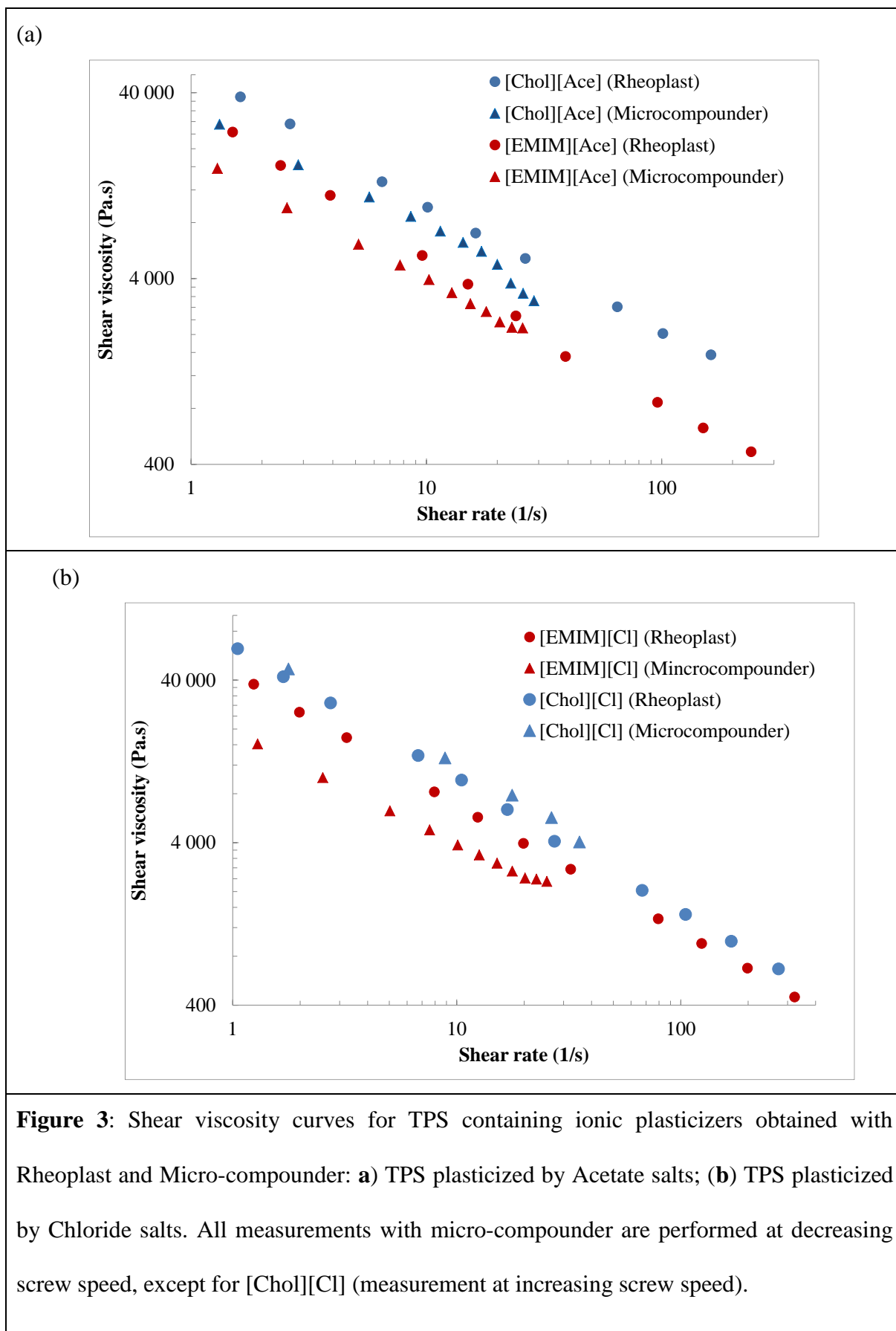


Figure 2: Reference shear viscosity curves: (a) Calibration of the Micro-compounder : Shear viscosity flow curves for polystyrene reference sample and Cross-Carreau model. (b) Shear viscosity flow curves for TPS plasticized by Glycerol with Rheoplast and Micro-compounder at 130°C (including measurements at decreasing screw speed and at increasing screw speed).



366 These results underline the need to examine more precisely the dependence of the viscosity
367 with processing variables and structural features:

- 368 • Surprisingly, when considering data from Rheoplast and Micro-compounder together,
369 no straightforward correlation appears between consistency values and SME (**Fig. 4a**).
370 However, for results obtained with Rheoplast, despite uncertainty on SME
371 measurement, it can be observed that K decreases with SME (**Fig. 4a**), in agreement
372 with the usual trend found in literature (Xie et al., 2012). Conversely, an increasing
373 trend is observed with SME in the case of the micro-compounder, once excluded the
374 values obtained for [Chol][CI] plasticized TPS, for the reasons discussed above. This
375 apparent contradiction arising from the opposite variations of K with SME may be
376 explained by considering how the thermomechanical treatment is applied to the product.
377 In the Rheoplast, the product is mechanically treated before measurement, therefore, the
378 more intense this treatment, the lower the viscosity of the plasticized starch melt.
379 Conversely, in the micro-compounder, the mechanical energy input increases during
380 measurements. Indeed, as explained in the experimental section, for the micro-
381 compounder, the SME values reported in **Table 1** and plotted in **Figure 4a** are obtained
382 for a series of experiments without rheological measurements and for a residence time
383 of 300 s, while in the rheological measurement take place for residence times from 150
384 s to 700 s. Therefore the viscosity is partly measured before the effective SME reaches
385 the value reported on **Fig. 4a**. Therefore, the more viscous the melt, the larger the SME
386 measured on the micro-compounder. This opposite trend qualifies the potential of the
387 micro-compounder as a rheometry tool for SME sensitive materials.
- 388 • The variations of consistency index K vs molar mass \overline{M}_w display an overall increasing
389 trend in the case of Rheoplast measurements (**Fig.4b**), obeying the rule of thumb “the
390 larger the polymer, the more viscous”. This trend is enhanced by the presence of

391 previous results obtained for maize starch, extruded in presence of water, for which K
392 was computed using the viscosity model proposed by (Vergnes & Villemaire, 1987) for
393 maize starch. However, significant dispersion is observed. Excluding again the values
394 obtained for [Chol][Cl], two dotted lines can be drawn as guides for the eyes: One with
395 higher slope for glycerol and Cholinium based RTILs, and one with lower slope for
396 imidazolium based RTILs, suggesting that the later lead to lower viscosities than the
397 former for similar starch macromolecular degradation.

398 • Indeed, the variations of consistency values vs glass transition temperature (**Fig. 4c**)
399 show a good correlation for results from both micro-compounder and Rheoplast, with
400 the rule of thumb “the more efficient the plasticizer, the lower the viscosity”. As
401 discussed previously, for \overline{M}_w above 10^6 g mol^{-1} the glass transition depends only on the
402 plasticizer (and water) present between polymer chains but is not expected to be
403 influenced by molar mass (Lafargue et al., 2007). The observed correlation between K
404 and T_g suggests that a similar trend applies for melt viscosity. Actually, the nature of
405 the plasticizer has a stronger influence than macromolecular degradation on shear
406 viscosity.

407

408

409

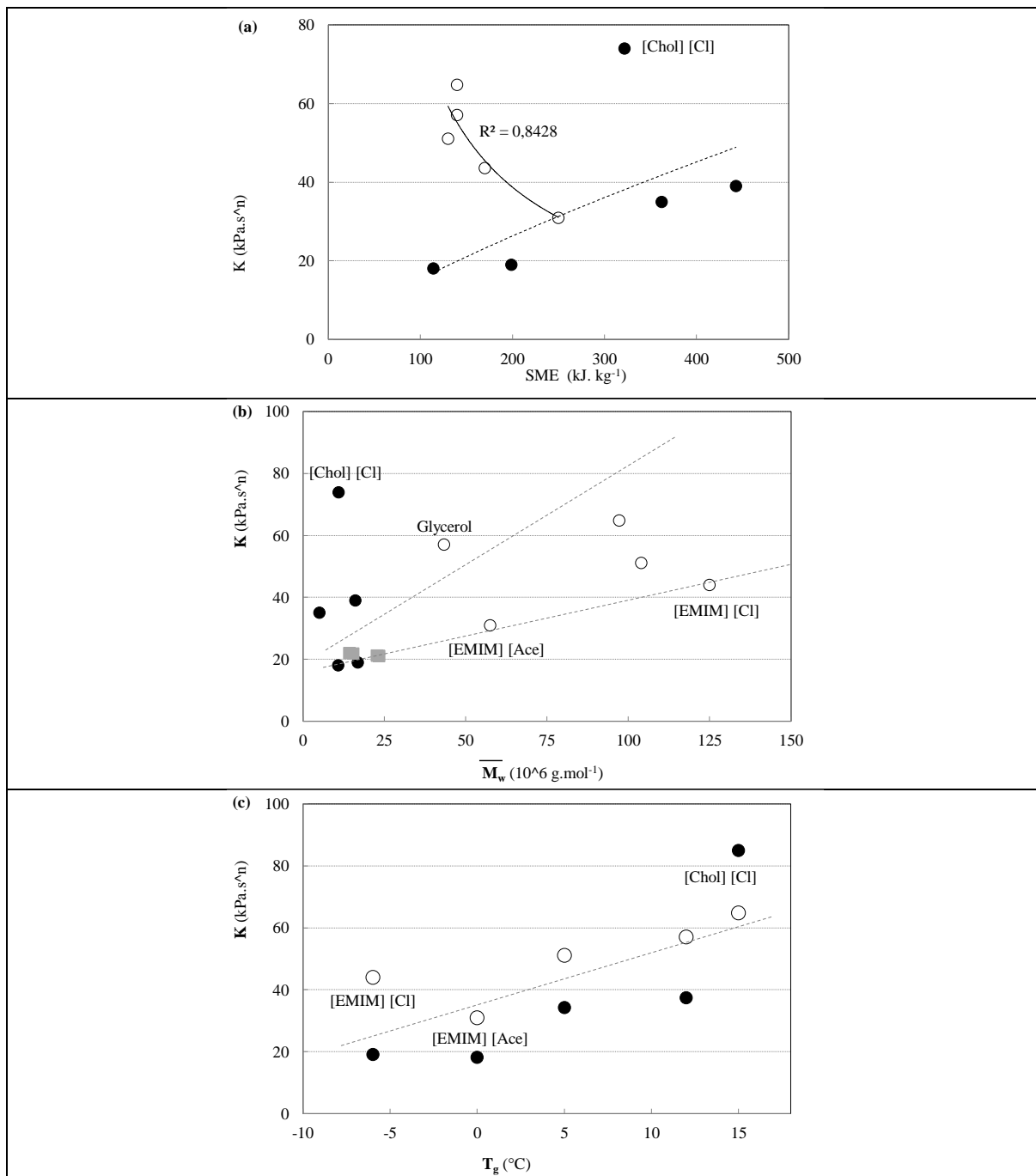


Figure 4: Variations of the consistency index (obtained with micro-compounder (●) and with Rheoplast (○)) with : (a) the SME (dotted line just show a trend whereas continuous line is the best fit for Rheoplast data) (b) the weight average molar mass \overline{M}_w (additional point for starch extruded in presence of water (■) (data from Baud et al., (Baud, Colonna, Della Valle, & Roger, 2001) , viscosity is computed using model from Vergnes & Villemaire (Vergnes & Villemaire, 1987), dotted line illustrates a trend). and (c) the glass transition temperature.

410 3.3) Extensional viscosity

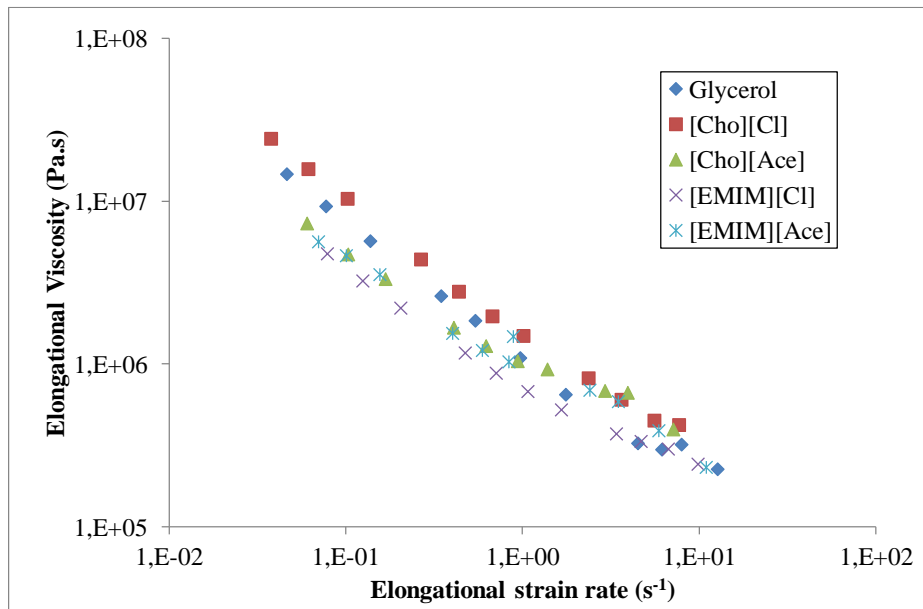
411 In addition to shear viscosity, the Rheoplast allows estimating the extensional viscous behavior
412 (**Fig.5**).

413 **Fig. 5a** shows the extensional viscosity flow curves obtained for each plasticized starch
414 formulation. The decreasing viscosity order is roughly the same as the one previously observed
415 for consistency values in **Table 2**, except for [EMIM][Ace] plasticized TPS. This plasticized
416 starch had the lowest shear viscosity values, but its extensional viscosity displays values among
417 the highest for extensional strain rate values larger than 1 s^{-1} . **Fig. 5b** shows the evolution of
418 the Trouton number defined as the ratio between extensional and shear viscosities, for equal
419 values of extensional strain and shear rates. All plasticized starches show Trouton numbers
420 significantly higher than the typical value of 3 for a Newtonian fluid. Ionic liquid plasticizers
421 also lead to higher values than for glycerol. Indeed, [EMIM][Ace] shows a unique behavior
422 with Trouton numbers as high as 50 due to its low shear viscosity combined with a high
423 extensional viscosity.

424 The comparison of extensional viscosity and Trouton number values also suggests that more
425 melt strength could be expected from Ionic liquid plasticized starches, and overall with
426 imidazolium acetate, which could perform better than glycerol TPS in processes, like film
427 blowing or foam manufacturing, where material stretching prevails (Munstedt, Steffl, &
428 Malmberg, 2005).

429

(a)



(b)

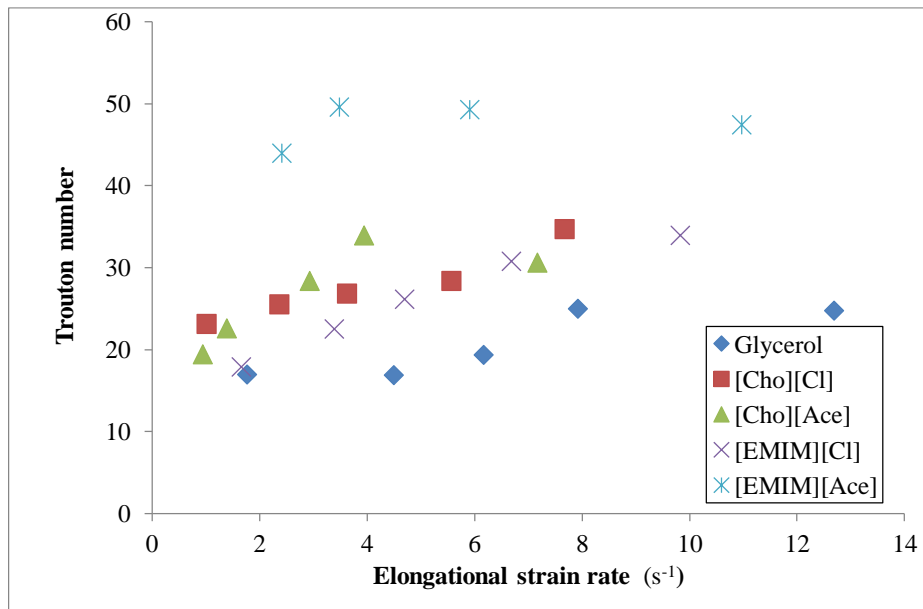


Figure 5: Extensional behavior of the plasticized starch: (a) extensional viscosity flow curves obtained with Rheoplast and (b) Trouton numbers.

433 4) Conclusion

434 In this work, maize starch was plasticized with different ionic plasticizers (Choline Chloride
435 and three room temperature ionic liquids) and glycerol used as a reference plasticizer. Two
436 different equipment allowing melt processing and rheological characterization have been used:
437 a micro-compounder and a capillary rheometer with pre-shearing. The shear viscosity of
438 plasticized starch was measured on both devices.

439 We have shown that, like for starches extruded in presence of water, significant macromolecular
440 degradation is obtained. Although this phenomenon induces a decrease of shear viscosity, it
441 does not account for all the variations of this rheological property. Indeed plasticizers have a
442 significant and specific action, as shown by their depressing effect on T_g . Indeed, the melt
443 consistency is found to better correlate to T_g than to the specific mechanical energy input or the
444 molar mass decrease due to processing.

445 The consistency values of the thermoplastic starches obtained for the different plasticizers, with
446 both Rheoplast and micro-compounder, rank in the same following order:

$$447 \quad K_{[\text{Chol}][\text{Cl}]} > K_{\text{Glycerol}} > K_{[\text{Chol}][\text{Ace}]} > K_{[\text{EMIM}][\text{Cl}]} > K_{[\text{EMIM}][\text{Ace}]}.$$

448 This agreement found for the viscosity results between both equipment suggest that micro-
449 compounder can be used to evaluate the plasticizing efficiency of ILs, all the more when small
450 quantities are available. Conversely, Rheoplast has confirmed to be an efficient mean to process
451 starchy material in similar but controlled conditions, like extrusion, whilst allowing an accurate
452 determination of shear viscosity and assessing extensional viscosity, all meaningful properties
453 for processing plasticized starches. Among all the tested ionic plasticizers 1-Ethyl-3-
454 methylimidazolium acetate ([EMIM][Ace]) is particularly promising since it leads to the lowest
455 shear viscosity, with limited macromolecular degradation and significantly higher Trouton
456 number values than for the other plasticizers.

457

458 **Acknowledgments**

459 We are grateful for the Financial support provided by the LIMPONAN project funded by the
460 “Région de Pays de la Loire” Council.

461

462 **References**

463 Abbott, A. P. (2009). Unpublished results presented at at the Royal Society Summer Science
464 Exhibition.

465 Averous, L. (2004). Biodegradable multiphase systems based on plasticized starch: A review.
466 *Journal of Macromolecular Science-Polymer Reviews*, C44(3), 231-274.

467 Barron, C., Bouchet, B., Della Valle, G., Gallant, D. J., & Planchot, V. (2001). Microscopical
468 study of the destructuring of waxy maize and smooth pea starches by shear and heat at
469 low hydration. *Journal of Cereal Science*, 33(3), 289-300.

470 Baud, C., Colonna, P., Della Valle, G., & Roger, P. (2001). *Determination of Macromolecular*
471 *degradation in physically modified starches. In Starch; Advances in Structure and*
472 *Function*. In T. L. Barsby, A. M. Donald, P. J. Frazier & p.-. Eds.; : (Eds.), (pp. pp 40-
473 44.). Cambridge, U.K.: Royal Society of Chemistry

474 Carriere, C. J. (1998). Evaluation of the entanglement molecular weights of maize starches from
475 solution rheological measurements. *Cereal Chemistry*, 75(3), 360-364.

476 Cogswell, F. N. (1972). Converging flow of polymer melts in extrusion dies. *Polymer*
477 *Engineering & Science*, 12(1), 64-73.

478 Colomines, G., Decaen, P., Lourdin, D., & Leroy, E. (2016). Biofriendly ionic liquids for starch
479 plasticization: a screening approach. *Rsc Advances*, 6(93), 90331-90337.

480 Cousin, T., Berto, C., Budtova, T., Kurek, J., & Navard, P. (2017). Influence of the Scale and
481 Type of Processing Tool on Plasticization of Cellulose Acetate. *Polymer Engineering*
482 *and Science*, 57(5), 563-569.

483 Decaen, P., Rolland-Sabate, A., Guilois, S., Jury, V., Allanic, N., Colomines, G., . . . Leroy, E.
484 (2017). Choline chloride vs choline ionic liquids for starch thermoplasticization.
485 *Carbohydrate Polymers*, 177, 424-432.

486 Della Valle, G., Vergnes, B., & Lourdin, D. (2007). Viscous properties of thermoplastic
487 starches from different botanical origin. *International Polymer Processing*, 22(5), 471-
488 479.

489 DellaValle, G., Boche, Y., Colonna, P., & Vergnes, B. (1995). The extrusion behaviour of
490 potato starch. *Carbohydrate Polymers*, 28(3), 255-264.

491 Gozzo, A., & Glittenberg, D. (2009). *Chapter 9.2 Starch: A Versatile Product from Renewable*
492 *Resources for Industrial Applications*. In *Sustainable Solutions for Modern Economies*
493 (pp. 238-263): The Royal Society of Chemistry

494 Horvat, M., Emin, M. A., Hochstein, B., Willenbacher, N., & Schuchmann, H. P. (2013). A
495 multiple-step slit die rheometer for rheological characterization of extruded starch
496 melts. *Journal of Food Engineering*, 116(2), 398-403.

497 Lafargue, D., Pontoire, B., Buleon, A., Doublier, J. L., & Lourdin, D. (2007). Structure and
498 mechanical properties of hydroxypropylated starch films. *Biomacromolecules*, 8(12),
499 3950-3958.

500 Leroy, E., Decaen, P., Jacquet, P., Coativy, G., Pontoire, B., Reguerre, A. L., & Lourdin, D.
501 (2012). Deep eutectic solvents as functional additives for starch based plastics. *Green*
502 *Chemistry*, 14(11), 3063-3066.

503 Leroy, E., Jacquet, P., Coativy, G., Reguerre, A. L., & Lourdin, D. (2012). Compatibilization
504 of starch-zein melt processed blends by an ionic liquid used as plasticizer. *Carbohydrate*
505 *Polymers*, 89(3), 955-963.

506 Liu, H. S., Xie, F. W., Yu, L., Chen, L., & Li, L. (2009). Thermal processing of starch-based
507 polymers. *Progress in Polymer Science*, 34(12), 1348-1368.

508 Liu, W. C., Halley, P. J., & Gilbert, R. G. (2010). Mechanism of Degradation of Starch, a Highly
509 Branched Polymer, during Extrusion. *Macromolecules*, 43(6), 2855-2864.

510 Logie, N., Della Valle, G., Rolland-Sabate, A., Descamps, N., & Soulestin, J. (2018). How does
511 temperature govern mechanisms of starch changes during extrusion? *Carbohydrate*
512 *Polymers*, 184, 57-65.

513 Martin, O., Averous, L., & Della Valle, G. (2003). In-line determination of plasticized wheat
514 starch viscoelastic behavior: impact of processing. *Carbohydrate Polymers*, 53(2), 169-
515 182.

516 Munstedt, H., Steffl, T., & Malmberg, A. (2005). Correlation between rheological behaviour in
517 uniaxial elongation and film blowing properties of various polyethylenes. *Rheologica*
518 *Acta*, 45(1), 14-22.

519 Ning, W., Yu, J. G., Ma, X. F., & Han, C. M. (2009). An Investigation of the Physical Properties
520 of Extruded Glycerol- and Formamide-Plasticized Cornstarch. *Journal of*
521 *Thermoplastic Composite Materials*, 22(3), 273-291.

522 Rolland-Sabate, A., Amani, N. G., Dufour, D., Guilois, S., & Colonna, P. (2003).
523 Macromolecular characteristics of ten yam (*Dioscorea* spp) starches. *Journal of the*
524 *Science of Food and Agriculture*, 83(9), 927-936.

525 Rolland-Sabate, A., Mendez-Montealvo, M. G., Colonna, P., & Planchot, V. (2008). Online
526 determination of structural properties and observation of deviations from power law
527 behavior. *Biomacromolecules*, 9(7), 1719-1730.

528 Sankri, A., Arhaliass, A., Dez, I., Gaumont, A. C., Grohens, Y., Lourdin, D., . . . Leroy, E.
529 (2010). Thermoplastic starch plasticized by an ionic liquid. *Carbohydrate Polymers*,
530 82(2), 256-263.

531 Sciarini, L. S., Rolland-Sabate, A., Guilois, S., Decaen, P., Leroy, E., & Le Bail, P. (2015).
532 Understanding the destructurement of starch in water-ionic liquid mixtures. *Green*
533 *Chemistry*, 17(1), 291-299.

534 Son, Y. (2007). Determination of shear viscosity and shear rate from pressure drop and flow
535 rate relationship in a rectangular channel. *Polymer*, 48(2), 632-637.

536 van den Einde, R. M., Akkermans, C., van der Goot, A. J., & Boom, R. M. (2004). Molecular
537 breakdown of corn starch by thermal and mechanical effects. *Carbohydrate Polymers*,
538 56(4), 415-422.

539 van den Einde, R. M., Bolsius, A., van Soest, J. J. G., Janssen, L., van der Goot, A. J., & Boom,
540 R. M. (2004). The effect of thermomechanical treatment on starch breakdown and the
541 consequences for process design. *Carbohydrate Polymers*, 55(1), 57-63.

542 Vergnes, B., Dellavalle, G., & Tayeb, J. (1993). A SPECIFIC SLIT DIE RHEOMETER FOR
543 EXTRUDED STARCHY PRODUCTS - DESIGN, VALIDATION AND
544 APPLICATION TO MAIZE STARCH. *Rheologica Acta*, 32(5), 465-476.

545 Vergnes, B., & Villemaire, J. P. (1987). RHEOLOGICAL BEHAVIOR OF LOW MOISTURE
546 MOLTEN MAIZE STARCH. *Rheologica Acta*, 26(6), 570-576.

547 Vergnes, B., Villemaire, J. P., Colonna, P., & Tayeb, J. (1987). INTERRELATIONSHIPS
548 BETWEEN THERMOMECHANICAL TREATMENT AND MACROMOLECULAR
549 DEGRADATION OF MAIZE STARCH IN A NOVEL RHEOMETER WITH
550 PRESHEARING. *Journal of Cereal Science*, 5(2), 189-202.

551 Wang, N., Yu, J. G., Chang, P. R., & Ma, X. F. (2007). Influence of citric acid on the properties
552 of glycerol-plasticized dry starch (DTPS) and DTPS/poly(lactic acid) blends. *Starch-*
553 *Starke*, 59(9), 409-417.

554 Willett, J. L., Jasberg, B. K., & Swanson, C. L. (1995). RHEOLOGY OF THERMOPLASTIC
555 STARCH - EFFECTS OF TEMPERATURE, MOISTURE-CONTENT, AND

556 ADDITIVES ON MELT VISCOSITY. *Polymer Engineering and Science*, 35(2), 202-
557 210.

558 Xie, F. W., Flanagan, B. M., Li, M., Sangwan, P., Truss, R. W., Halley, P. J., . . . McNally, T.
559 (2014). Characteristics of starch-based films plasticised by glycerol and by the ionic
560 liquid 1-ethyl-3-methylimidazolium acetate: A comparative study. *Carbohydrate*
561 *Polymers*, 111, 841-848.

562 Xie, F. W., Halley, P. J., & Averous, L. (2012). Rheology to understand and optimize
563 processibility, structures and properties of starch polymeric materials. *Progress in*
564 *Polymer Science*, 37(4), 595-623.

565 Yousfi, M., Alix, S., Lebeau, M., Soulestin, J., Lacrampe, M. F., & Krawczak, P. (2014).
566 Evaluation of rheological properties of non-Newtonian fluids in micro rheology
567 compounder: Experimental procedures for a reliable polymer melt viscosity
568 measurement. *Polymer Testing*, 40, 207-217.

569 Zdanowicz, M., & Szychaj, T. (2011). Ionic liquids as starch plasticizers or solvents. *Polimery*,
570 56(11-12), 861-864.

571